

Critical Considerations for Helicopters During Runway Takeoffs

Yiyuan Zhao*

University of Minnesota, Minneapolis, Minnesota 55455

and

Robert T. N. Chen†

NASA Ames Research Center, Moffett Field, California 94035

This article presents optimal runway takeoff trajectories of a multiengine helicopter in the event of one engine failure. A point-mass model representative of the UH-60A helicopter is employed. Pilot response delays are ignored. Two optimal control problems are formulated for both continued takeoff and rejected takeoff after a single engine failure. Subject to specified safety conditions, the first formulation minimizes the runway length required for a given takeoff weight, whereas the second maximizes the takeoff weight for a given runway length in continued takeoff and for an unspecified runway length in rejected takeoff. Constraints on thrust angle, and thrust magnitude are included. For the continued takeoff, an optimal choice of the takeoff safety speed is determined to be about 15 ft/s above the initial airspeed at engine failure. Maximum takeoff weight is dictated by the remaining power after one engine failure if the runway length is sufficient, and is determined by the available runway length otherwise. For the rejected takeoff, the minimum runway length is a function of initial conditions at engine failure, and is roughly independent of takeoff weights. These results replicate some key characteristics of those from flight tests reported in the literature.

Nomenclature

C_P	= power coefficient
C_T	= thrust coefficient
(C_x, C_z)	= (horizontal, vertical) component of thrust coefficient
c_d	= mean blade profile drag coefficient
D_f	= parasite drag of the fuselage
f_e	= equivalent flat plate area of the fuselage
f_G	= ground effect factor
g	= acceleration of gravity
h	= helicopter altitude
I_R	= polar moment of inertia of the main rotor
K_{ind}	= induced power factor
m	= helicopter mass
m_0	= reference mass
P_{OEI}	= power available in one engine inoperative
P_{pr}	= main rotor profile power
P_{req}	= helicopter power required
R	= main rotor radius
T	= main rotor thrust
\bar{U}_c	= main rotor climb velocity component
\bar{U}_t	= tangent velocity component on the main rotor
U_2	= horizontal component of takeoff safety speed
(u, w)	= (horizontal, vertical) component of inertial velocity
u_1, u_2	= normalized helicopter controls
V_{TOSS}	= takeoff safety speed
V_Y	= airspeed for best rate of climb

\bar{v}_i	= normalized main rotor induced velocity
(X_{CTO}, X_{RTO})	= total runway length in (continued takeoff, rejected takeoff)
x	= helicopter horizontal location
$(x_{f,cto}, x_{f,rto})$	= airborne runway required from optimization in (continued takeoff, rejected takeoff)
x_i	= normalized helicopter states, $i = 1, \dots, 5$
β	= thrust inclination angle
γ	= flight-path angle
δ	= ratio of reference mass to actual mass
η	= helicopter power efficiency factor
ρ	= air density
σ	= main rotor solidity ratio
τ	= normalized time
Ω	= main rotor angular speed

I. Introduction

FEDERAL Aviation Regulation Part 29 specifies that transport helicopters must be certificated as either category A or B.¹ Category-B certification applies to either single or multiengine helicopters with gross weight less than 20,000 lb. A Category-B helicopter must be able to land safely in the case of one or all engine failures. There is no requirement, however, for continued flight capability.

In contrast, Category-A certification applies to multiengine helicopters with independent engine systems. It requires that helicopters be able to continue the flight with one engine inoperative (OEI). Therefore, Category-A helicopters are permitted to operate from rooftops and oil rigs, and to fly to areas where no emergency landing sites are available. Specifically, in takeoff flights (Fig. 1), the pilot must continue the takeoff (CTO) if one engine fails after the helicopter has passed the takeoff decision point (TDP), and should land, or reject the takeoff (RTO), if the engine failure occurs before reaching TDP. While there is no maximum weight limit, a Category-A helicopter must be able to satisfy OEI operation requirements within the available runway field.

To date, Category-A flight procedures have been determined from flight tests, which can be dangerous, very time-

Received July 17, 1994; presented as Paper 94-3695 at the AIAA Guidance, Navigation, and Control Conference, Scottsdale, AZ, Aug. 1–3, 1994; revision received Dec. 19, 1994; accepted for publication Jan. 10, 1995. Copyright © 1995 by the American Institute of Aeronautics and Astronautics, Inc. All rights reserved.

*Assistant Professor, Department of Aerospace Engineering and Mechanics. Member AIAA.

†Civil Rotorcraft Group Leader, Rotorcraft and Powered Lift Branch.

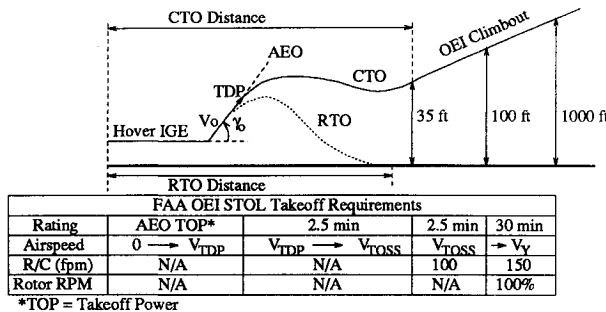


Fig. 1 Category-A helicopter runway (or STOL) takeoff procedure.

consuming, and costly. Flight manual instructions based on flight tests provide the pilot with very conservative recommendations in terms of maximum takeoff weight or required runway length. Usually, a single TDP is recommended for all flight conditions. The pilot cannot trade reduced takeoff weight or favorable ambient conditions for a shorter runway.

Recently, several investigators studied a variable TDP velocity concept. Cerbe and Reichert² developed a quasistationary simulation model based on the power required data field and conducted parameter optimizations. They discussed the relationship between the TDP velocity and the takeoff safety speed V_{ROSS} in a runway takeoff for the B0 105 helicopter. Saal and Cole³ conducted an extensive flight investigation with the S-76B helicopter and proposed varying TDP velocity and V_{ROSS} to provide flexibility for optimizing payload and field lengths in a runway takeoff. Okuno and Kawachi⁴ applied optimal control theory and studied choices of TDP velocity and takeoff slope for runway length reduction. In addition, Vodegel and Stevens⁵ developed a computer program to simulate Category-A vertical takeoff flights. Goldenberg et al.⁶ developed a sideway ascent/descent operation procedure on an elevated helipad for the Model 230 helicopter. This procedure was previously discussed by Lande.⁷ Optimal control theories have also been used to study landing procedures in autorotation after all engines fail.⁸⁻¹⁰

The main objective of this article is to understand the effects of fundamental parameters associated with Category-A runway takeoff operations. There are three primary concerns in a Category-A runway takeoff: 1) runway field length, 2) payload capability, and 3) safety. Any good flight strategy must achieve a proper balance among these three factors.

In this article, a point-mass helicopter model is used and two nonlinear optimal control problems are formulated for both the continued takeoff and the rejected takeoff. Under specified safety conditions, the first formulation minimizes the required runway length for a given takeoff weight, while the second formulation maximizes the takeoff weight for a specified runway length in CTO and for an unspecified runway length in RTO. Both formulations are subject to maximum and minimum rotor speed constraint, and thrust magnitude and angle constraints.

To select a proper TDP, conditions at the single engine failure are systematically varied. These conditions are used as the initial conditions in trajectory optimizations. Based on combined considerations of continued takeoff and rejected takeoff, one can select suitable TDPs that provide overall minimum runway lengths.

II. Helicopter Model and Equations of Motion

A. Point-Mass Helicopter Model

A two-dimensional point-mass helicopter model^{8,9} is used for the present study. Figure 2 shows the force balance in the point-mass model. The main rotor thrust can be expressed in terms of its coefficient C_T :

$$T = \rho(\pi R^2)(\Omega R)^2 C_T \quad (1)$$

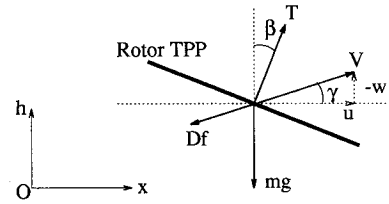


Fig. 2 Point-mass helicopter model.

Fuselage drag can be expressed as

$$D_f = -\frac{1}{2}\rho f_e V(ui + wj) \quad (2)$$

The two-dimensional equations of motion are therefore given by

$$m\dot{u} = T \sin \beta - \frac{1}{2}\rho f_e u \sqrt{u^2 + w^2} \quad (3)$$

$$m\dot{w} = T \cos \beta - \frac{1}{2}\rho f_e w \sqrt{u^2 + w^2} + mg \quad (4)$$

$$\dot{x} = u \quad (5)$$

$$\dot{h} = -w \quad (6)$$

The airspeed and flight-path angle are

$$V = \sqrt{u^2 + w^2} \quad (7)$$

$$\sin \gamma = -(w/V) \quad (8)$$

The rotor rotational acceleration is given by¹¹

$$\begin{aligned} I_R \Omega \dot{\Omega} &= P_{OEI} - P_{req} \\ &= P_{OEI} - \frac{1}{\eta} [\rho(\pi R^2)(\Omega R)^3] C_P \end{aligned} \quad (9)$$

where the efficiency factor η accounts for the power losses associated with tail rotor and transmission.¹²

Category-A OEI operations are basically a power deficiency problem. The power from the remaining engine(s) after one engine becomes inoperative is crucial. There are two types of power ratings: 1) all engine operating (AEO) power ratings and 2) OEI contingency power ratings. AEO power ratings consist of AEO takeoff power and maximum continuous power. The OEI takeoff contingency power ratings are defined in terms of the level and the duration, which include a 2.5-min power rating and a 30-min power rating. (A 30-s supercontingency power rating is also being proposed.¹³) In the current study, we assume that the 2.5-min OEI power rating is 110% of the AEO takeoff power rating, while the 30-min OEI power rating is 105% of the AEO takeoff power rating. These are typical based on existing engine data. Therefore,

$$P_{OEI} = (110 \text{ or } 105\%)(\text{AEO takeoff rating}/2) - P_{accessory} \quad (10)$$

The main rotor power required in Eq. (9) is a sum of the induced power, climb power, and the profile power:

$$C_P = C_T \sqrt{(C_T/2)} (K_{ind} f_G \bar{v}_i + \bar{U}_c) + C_{P_{pr}} \quad (11)$$

In this article, it is assumed that $f_G = 1$ and $K_{ind} = 1.15$.

To determine the normalized rotor-induced velocity \bar{v}_i , two normalized velocity components on the rotor are defined as

$$\bar{U}_c = \frac{u \sin \beta - w \cos \beta}{\Omega R \sqrt{C_T/2}} \quad (12)$$

$$\bar{U}_i = \frac{w \sin \beta + u \cos \beta}{\Omega R \sqrt{C_T/2}} \quad (13)$$

Outside the vortex-ring state

$$(2\bar{U}_c + 3)^2 + \bar{U}_i^2 > 1 \quad (14)$$

the rotor-induced velocity can be described by the momentum theory^{14–16}:

$$\bar{v}_i^4 + 2\bar{U}_c\bar{v}_i^3 + (\bar{U}_c^2 + \bar{U}_i^2)\bar{v}_i^2 = 1 \quad (15)$$

which can be solved efficiently with a Newton–Raphson scheme. In the vortex-ring state

$$(2\bar{U}_c + 3)^2 + \bar{U}_i^2 \leq 1 \quad (16)$$

Johnson⁸ proposed an empirical formula:

$$\bar{v}_i = \bar{U}_c(0.373\bar{U}_c^2 + 0.598\bar{U}_i^2 - 1.991) \quad (17)$$

In the vortex-ring state, the actual induced flow is often unsteady and erratic. Therefore, the induced velocity in Eq. (17) should only be interpreted as the mean value affecting the induced power.

For takeoff and landing flights, the profile power is expressed by¹⁴

$$C_{P_{pr}} \approx \frac{1}{8}\sigma c_d \quad (18)$$

B. Constraints

Thrust coefficient and thrust angle must satisfy

$$0 \leq C_T \leq C_{T_{\max}} |\beta| \leq \beta_{\max} \quad (19)$$

The rotor angular speed is constrained by upper and lower limit

$$\Omega_{\min} \leq \Omega \leq \Omega_{\max} \quad (20)$$

Specific terminal constraints depending on the type of OEI flight are discussed later.

C. Equations for Trajectory Optimization

In practice, the pilot controls the rotor flapping motion of a helicopter through collective pitch and cyclics. The flapping motion is usually much faster than both the helicopter rigid-body motion and the trajectory motion. Desired levels of rotor thrust magnitude and direction can be achieved almost instantaneously by applying proper collective and cyclic controls. Therefore, the horizontal and the vertical components of the thrust coefficient can be considered as the control variables:

$$C_x = C_T \sin \beta \quad (21)$$

$$C_z = C_T \cos \beta \quad (22)$$

where the thrust coefficient is defined in Eq. (1).

Proper choice and scaling of variables are vital to a successful convergence of an optimization problem. Consequently, all distances are normalized judiciously by $(10R)$ and time by $100/\Omega_0$, where Ω_0 is the nominal rotor speed. Define

$$x_1 = \frac{w}{0.1\Omega_0 R} \quad x_2 = \frac{u}{0.1\Omega_0 R} \quad x_3 = \frac{\Omega}{\Omega_0} \triangleq \bar{\Omega} \quad (23)$$

$$x_4 = \frac{h}{10R} \quad x_5 = \frac{x}{10R} \quad \tau = \frac{\Omega_0 t}{100} \quad (24)$$

$$u_1 = 10^3 C_z \quad u_2 = 10^3 C_x \quad (25)$$

From Eqs. (3–6) and Eq. (9), we have

$$x'_1 = \tau_f(g_0 - \delta\rho_0 x_3^2 u_1 - \delta f_0 x_1 \sqrt{x_1^2 + x_2^2}) \quad (26)$$

$$x'_2 = \tau_f \delta(\rho_0 x_3^2 u_2 - f_0 x_2 \sqrt{x_1^2 + x_2^2}) \quad (27)$$

$$x'_3 = \tau_f [(p_s/x_3) + i_0 x_3 (x_1 u_1 - x_2 u_2) - k_p x_3^2 - k_i x_3^2 (u_1^2 + u_2^2)^{3/4} \bar{v}_i] \quad (28)$$

$$x'_4 = -\tau_f x_1 \quad (29)$$

$$x'_5 = \tau_f x_2 \quad (30)$$

where the prime represents differentiation with respect to (τ_f) , and the coefficients are given:

$$g_0 = \frac{1000g}{\Omega_0^2 R}, \quad \rho_0 = \frac{\rho\pi R^3}{m_0}, \quad f_0 = \frac{5\rho f_c R}{m_0}, \quad p_s = \frac{100P_{OEI}}{I_R \Omega_0^3}$$

$$i_0 = \frac{\rho\pi R^5}{100\eta I_R}, \quad k_p = 1250\sigma c_d i_0, \quad k_i = i_0 \frac{K_{ind}}{\sqrt{20}}$$

$$\delta = m_0/m \quad (31)$$

The final time is computed from

$$t_f = 100\tau_f/\Omega_0 \quad (32)$$

Inequality constraints in Eqs. (19) and (20) can be enforced using

$$u_2 \leq (\tan \beta_{\max}) u_1 \quad (33)$$

$$u_2 \geq -(\tan \beta_{\max}) u_1 \quad (34)$$

$$x_3 \leq \bar{\Omega}_{\max} \quad (35)$$

$$x_3 \geq \bar{\Omega}_{\min} \quad (36)$$

The maximum thrust coefficient is always satisfied in the optimal trajectories.

D. Example Helicopter: UH-60A

The Sikorsky UH-60A (Black Hawk) helicopter^{17–20} is used as the example helicopter. This single rotor helicopter is powered by two T700-GE-700 turboshaft engines. The Appendix lists some important parameters of this helicopter compiled from Howlett¹⁸ and Prouty,¹⁹ as well as parameters used in the optimization studies.

III. Numerical Studies

A. Nominal AEO Runway Takeoff Path

For AEO runway takeoffs, Schmitz²¹ recommended a simple strategy that maximizes payload over a given runway length and a specified obstacle height. Following his strategy, a helicopter would start the takeoff with hover in ground effect, accelerate horizontally to a specified rotation speed, and then climb at a constant airspeed V_0 and a constant flight path angle γ_0 (Fig. 1).

For the current study of Category-A runway takeoff, we specify the following ground rules. A helicopter begins takeoff with a hover in ground effect at 5 ft. The helicopter then accelerates horizontally at 0.2 g until $V = V_0$. At V_0 , the helicopter starts climbing at a constant flight path angle γ_0 while maintaining the constant airspeed. For RTO, the helicopter decelerates at -0.2 g from touchdown to a complete stop.

The following discrete values of nominal AEO takeoff airspeed V_0 and flight-path angle γ_0 are used for the example helicopter:

$$V_0 = 50, 65, 80 \text{ ft/s} \quad (37)$$

$$\gamma_0 = 3, 5, 7, 9, 11 \text{ deg} \quad (38)$$

For each set of (V_0, γ_0) , the following values of engine failure height h_0 are investigated:

$$h_0 = 10, 15, 20, 25, 30 \text{ ft} \quad (39)$$

The range of airspeed is selected to take advantage of ground effect²² and to avoid the unreliable pitot-static tube performances when airspeed is below 30 kn. The range of flight-path angle is selected so that the corresponding change in potential energy is comparable to that in kinetic energy.

B. Solution Parameters and Strategies

Definition of a Category-A runway takeoff strategy requires the determination of many parameters including TDP conditions (Fig. 1). Usually, TDP is specified by airspeed and altitude. Because Category-A operations are power deficiency problems, both energy state and energy rate of a helicopter at the point of engine failure are important. Therefore, the choice of a nominal AEO takeoff path affects TDP conditions. For the nominal AEO takeoff path selected previously, the TDP conditions ought to be specified in terms of $(h_{\text{TDP}}, V_0, \gamma_0, \Omega_0)$. In addition, the takeoff safety speed V_{TOSS} in CTO, limits of acceptable touchdown velocity components in RTO, and levels of constraints, all affect the maximum takeoff weight and required runway length. Furthermore, ambient atmospheric conditions affect helicopter OEI performance.

In this article, we limit the varying parameters to V_0 , γ_0 , h_{TDP} , V_{TOSS} , and W_{max} . Other parameters are judiciously selected and fixed in the course of optimizations. However, methods developed in this article can be used equally well for studying effects of other parameters such as OEI power levels and the polar moment of inertia of the rotor.

Of primary concern in Category-A runway takeoff operations are runway field length, payload, and safety. Clearly, tradeoffs must be made among maximizing payload capability, minimizing required runway field length, and maximizing safety. Flight manual instructions are often conservatively safe. In this article, therefore, we determine flight paths that minimize runway field lengths and maximize payload capabilities, subject to safety levels and performance standards specified in the FAA regulations. As a result, the problem becomes one of determining V_0 , γ_0 , h_{TDP} , V_{TOSS} , and W_{max} to minimize overall required runway field length and to maximize payload capability of a helicopter during OEI operations.

A complete solution to the Category-A runway takeoff problem consists of three segments: 1) OEI climbout, 2) continued takeoff, and 3) rejected takeoff (Fig. 1). In this article, we study each segment separately and combine them to determine overall optimum strategies.

1) The OEI climb requirements determine the maximum takeoff weight meaningful for the whole Category-A operation. Therefore, maximum takeoff weights in the OEI climbout are first examined using steady-state equations.

2) We then study continued takeoff and rejected takeoff separately. Nonlinear optimal control problems are formulated to minimize runway lengths and to maximize payload capabilities.

3) Finally, minimum runway lengths for CTO and RTO are compared to yield overall minimum runway field lengths for Category-A runway operations. Details follow in Secs. IV, V, and VI.

C. Numerical Solution Techniques for Trajectory Optimizations

Conditions at engine failure point on a nominal AEO takeoff path are used as the initial conditions for trajectory optimizations. To obtain numerical solutions, all the inequality constraints are transformed into equality constraints using a slack variable method.²³ The “sequential gradient restoration algorithm” by Miele et al.²⁴ is then employed.

Different initial guesses of states, controls, and parameters are tried for trajectory optimizations. In this article, we assume initially that all state variables are constant and equal to their corresponding initial-time values, and all control variables are constant as well. Convergence criteria are selected such that further iterations will not change the performance indices by more than 0.5%.

IV. Continued Takeoff Flight

Federal Aviation Administration (FAA) rules for OEI continued takeoff have two parts.¹ During the transition flight from one engine failure to the beginning of OEI climbout, a helicopter must attain a minimum altitude of 35 ft and the takeoff safety speed V_{TOSS} , which assures a minimum climb rate of 100 fpm. If U_2 is the horizontal component of the takeoff safety speed

$$V_{\text{TOSS}} = \sqrt{U_2^2 + (1.667)^2} \approx U_2 \quad (40)$$

During the subsequent OEI climbout phase, the helicopter must be able to satisfy the OEI climb requirements with the remaining power available (Fig. 1). These OEI requirements determine maximum weights possible for given OEI powers and flight speeds.

A. Maximum Weight in Steady OEI Climb

There are two segments in the OEI climbout. From 35 ft to at least 100 ft, the helicopter must be able to maintain a minimum rate of climb of 100 fpm at V_{TOSS} with the 2.5-min OEI power. From 100 to 1000 ft, the helicopter must be able to accelerate from V_{TOSS} to V_Y and achieve a minimum climb rate of 150 fpm at V_Y with the 30-min OEI power.

While the maximum power available is nearly constant, the power requirement of a helicopter varies with the speed of flight. As a result, maximum weight possible in an OEI climb depends on the speed of flight. Figure 3 shows the maximum weight as a function of the horizontal velocity component U_2 in a steady climb.

Figure 3 is obtained from the steady-state solutions of Eqs. (26–28), with three sets of conditions: 1) $P_{\text{OEI}} = 110\%$ AEO takeoff power, rate of climb is 100 fpm, and $\Omega = 1.0$; 2) $P_{\text{OEI}} = 110\%$, rate of climb is 100 fpm, and $\Omega = 0.91$; and 3) OEI power is 105% of AEO takeoff power, the rate of climb is 150 fpm, and $\Omega = 1.0$.

The maximum weight increases as U_2 increases and achieves a peak value at V_Y . This is consistent with the typical helicopter power requirement. To be able to carry a higher payload in the OEI climb, the helicopter must attain a larger speed U_2 (or V_{TOSS}) at the end of the transition flight.

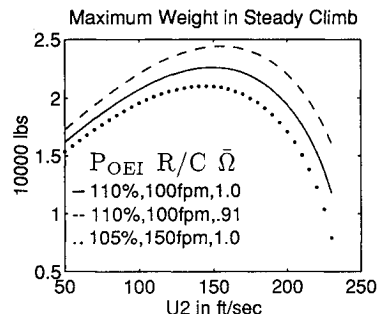


Fig. 3 Maximum weight in steady OEI climb.

Table 1 Maximum weight in steady OEI climb

U_2 , fps	W, lb
55	16,698
60	17,211
65	17,715
70	18,206
75	18,681
80	19,137
85	19,572
90	19,984
95	20,372
100	20,734

In the current study, U_2 covers the range of $55 \leq U_2 \leq 100$ ft/s. Figure 3 shows that $V_Y \approx 150$ ft/s. A helicopter flying at V_Y with 105% P_{OEI} can carry more weight than at any U_2 in this range with 110% P_{OEI} . Therefore, the first climb segment is more restrictive. Consequently, we determine maximum weights from the requirements of the first OEI climb segment. Table 1 lists maximum takeoff weights at several U_2 values determined from the first climb segment corresponding to $P_{OEI} = 110\%$ AEO takeoff power, climb rate of 100 fpm, and $\Omega = 1.0$.

B. Minimum Runway Length Problem

The minimum runway continued takeoff problem minimizes

$$I = x_5(\tau_f) \quad (41)$$

subject to Eqs. (26–36), and the following terminal constraints:

$$h(\tau_f) = 35 \text{ ft} \quad (42)$$

$$-w(\tau_f) \geq 100 \text{ fpm} = 1.667 \text{ fps} \quad (43)$$

$$u(\tau_f) = U_2 \quad (44)$$

where Eq. (44) is added to provide consistency between the transition CTO flight and the OEI climb. In the FAA regulations, V_{TOSS} is implicitly specified to assure a minimum climb rate of 100 fpm. Preliminary optimization studies indicate that the climb rate of 100 fpm can be achieved with different airspeeds. On the other hand, a certain maximum weight in a steady OEI climb is directly related to a certain steady speed in the climb, as was shown previously.

There is a tradeoff in selecting U_2 . A larger U_2 leads to a higher takeoff weight in the steady OEI climb, but requires a longer runway during the transition flight. To determine proper values of U_2 , we compare the optimal trajectories for

$$\Delta V = U_2 - V_0 = 5, 10, 15, 20 \text{ ft/s} \quad (45)$$

For each U_2 , the takeoff weight is obtained from Table 1. Figure 4 shows the altitude, airspeed, and helicopter power required histories for different U_2 , for $V_0 = 50$ ft/s, $\gamma_0 = 5$ deg, and an engine failure height of $h_0 = 20$ ft. Optimal trajectories for other engine failure heights and/or different V_0 show a similar trend.

Figure 4 shows that the largest takeoff safety speed (thus, the largest payload, Table 1) without any altitude decrease corresponds to $U_2 = 65$ ft/s. Therefore, we recommend that $U_2 = V_0 + 15$ ft/s. This result is consistent with flight manual instructions of the Supa Puma helicopter.²⁵ Saal and Cole also recommended a 10-kn difference between V_{TOSS} and V_0 for achieving balanced field lengths.³

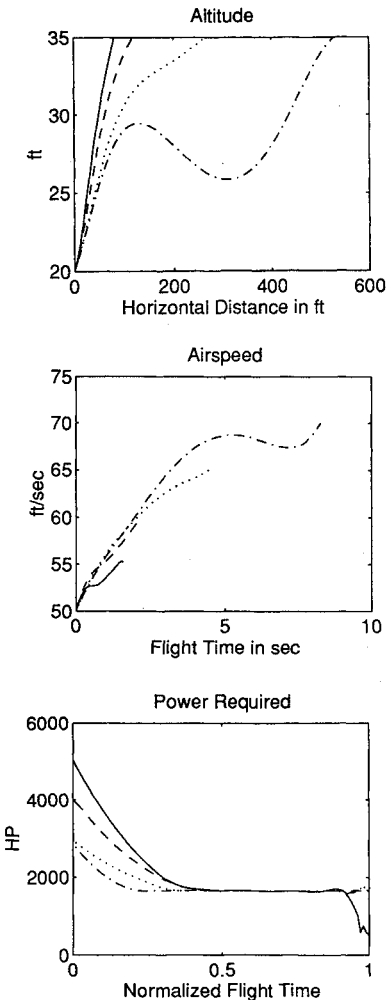


Fig. 4 Effect of U_2 in OEI minimum runway length CTO.

Figure 5 shows time histories of other states and controls in CTO with $V_0 = 50$ ft/s, $\gamma_0 = 5$ deg, $h = 20$ ft, and different values of U_2 . In all cases, the rotor angular speed reduces to and stays at the lower limit. The helicopter power required P_{req} reduces from its initial value to a steady-state value, which is equal to the OEI power available. Therefore, a typical continued takeoff consists of three phases. Initially, the helicopter reconfigures itself so that the helicopter power required quickly matches the power available and main rotor speed reduces to the lower limit. The helicopter trades the rotational energy of its rotor for potential and kinetic energy. During the second phase, the helicopter power required is maintained at the OEI power level and the rotor speed is maintained at the lower limit while the helicopter gains airspeed and altitude. Finally, the helicopter exchanges different energy sources to achieve the terminal conditions. During the whole flight, the helicopter always stays out of the vortexing state.

Due to the inequality constraint of Eq. (43), the final climb rate is either equal to or above 100 fpm. For a larger U_2 and/or a lower engine failure height h_0 , Eq. (43) is usually satisfied as an equality, or the final climb rate is roughly equal to 100 fpm. For a smaller U_2 and/or a higher h_0 , the final climb rate is often above 100 fpm. For simplicity, we can enforce Eq. (43) as an equality in all cases. The resulting optimal trajectories require only slightly longer runway lengths than those using the strict inequality of Eq. (43).

The British Civil Aviation Authority (CAA) issues a different set of standards for Category-A continued takeoff flight.³ A helicopter becoming OEI after TDP must achieve a min-

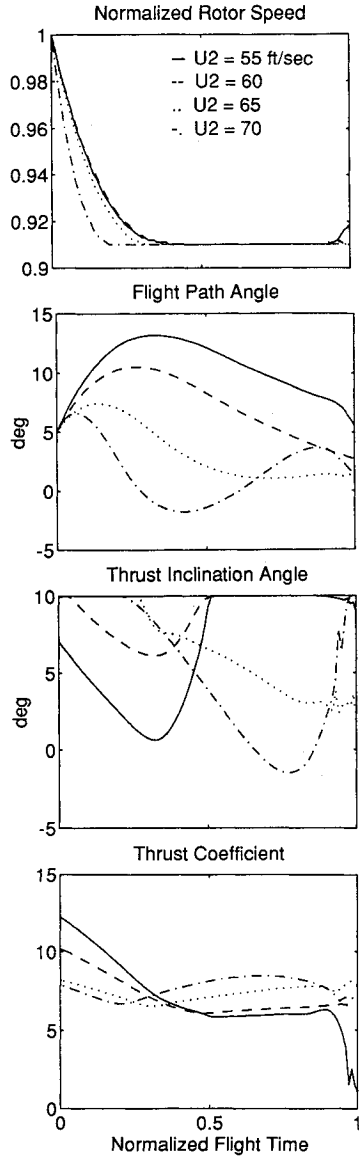


Fig. 5 Minimum runway length CTO with $V_0 = 50$ ft/s, $\gamma_0 = 5$ deg, $h_0 = 20$ ft, and U_2 varying from 55 to 70 ft/s.

imum altitude of 50 ft, a minimum climb rate of 100 fpm, and a minimum climb gradient of 3%. Mathematically

$$h(\tau_f) = 50 \text{ ft} \quad (46)$$

$$-w(\tau_f) \geq 100 \text{ fpm} \quad (47)$$

$$-w(\tau_f) \geq 0.03u(\tau_f) \quad (48)$$

$$u(\tau_f) = U_2 \quad (49)$$

where the last constraint is again added for consistency between the transition CTO flight and the steady OEI climb. Clearly, meeting the requirement of Eq. (47) automatically satisfies Eq. (48) if $U_2 \leq 55.56$ ft/s, and vice versa if $U_2 > 55.56$ ft/s. Therefore, only one of Eqs. (47) and (48) needs to be included in the optimizations.

Figure 6 compares the helicopter altitude and airspeed following FAA rules and CAA rules for the same engine failure conditions: $V_0 = 50$ ft/s, $\gamma_0 = 5$ deg, $U_2 = 65$ ft/s, $W = 17,715$ lb. The helicopter traces almost the same path for altitude up to 35 ft. Therefore, for the example helicopter, there is no fundamental difference between the two sets of rules, other than that the CAA rules require a runway length

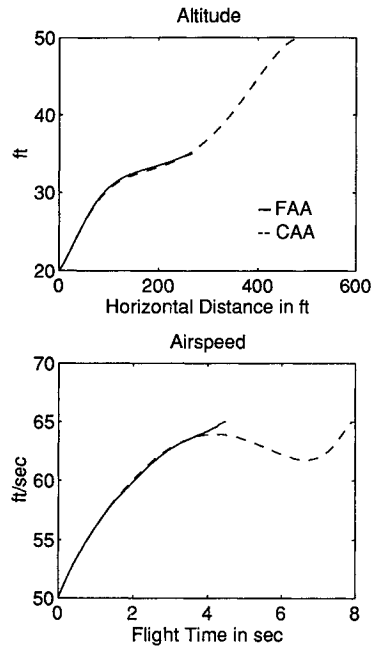


Fig. 6 Minimum runway length CTO with FAA and CAA rules, $V_0 = 50$ ft/s, $\gamma_0 = 5$ deg, and $U_2 = 65$ ft/s.

twice as long as the FAA rules. Whether the stringent CAA rules are justified depends on the conditions of surrounding obstacles. If not explicitly stated, all results in this article are obtained with FAA rules.

C. Maximum Takeoff Weight in Transition Flight

In a related problem, we can maximize the takeoff weight for a specified runway length

$$\min I = \delta \quad (50)$$

subject to Eqs. (26–36), Eqs. (42–44), and

$$x(\tau_f) = X_{\text{specified}} \quad (51)$$

It turns out that this problem is a dual of the minimum runway problem for a given takeoff weight. In other words, the specified takeoff weight in the minimum runway length problem is equal to the solution of the maximum weight problem if the minimum runway length in the first problem is specified in the second problem. Optimal trajectories from the two problems are nearly identical.

As the specified runway length decreases, the maximum weight in the transition CTO flight also decreases. As a result, the maximum takeoff weight in OEI CTO is determined by steady OEI climb requirements if the runway length is sufficiently long, and is determined by the available runway length otherwise. Details are omitted.

Sometimes, a helicopter carries less weight than the maximum OEI weight possible. There are two ways to study the less-weight scenario optimally. We can find the U_2 from Table 1 corresponding to the given weight and minimize the runway length with this U_2 . Alternatively, we can fix $U_2 = V_0 + 15$ and minimize the runway length for whatever weight given. The second approach offers consistency for different takeoff weights, since the pilot does not have to remember which U_2 to follow.

Optimal trajectories are computed to minimize lengths for three takeoff weights with $U_2 = V_0 + 15$ ft/s, $V_0 = 50$ ft/s, and $h_0 = 20$ ft. Results show that the helicopter can easily carry less weights and require shorter runway lengths. Details are omitted.

V. Rejected Takeoff Flight

If an engine failure occurs before the helicopter reaches TDP, the pilot must land the helicopter, or reject the takeoff. In a safe rejected takeoff, the helicopter must achieve reasonable touchdown speeds:

$$h(\tau_f) = 0 \quad (52)$$

$$w(\tau_f) \leq w_{\max} \quad (53)$$

$$u(\tau_f) \leq u_{\max} \quad (54)$$

A. Minimum Runway Length Problem

A minimum runway RTO problem minimizes the final horizontal distance as in Eq. (41), subject to Eqs. (26–36), and terminal constraints in Eqs. (52–54).

The most remarkable feature of the minimum runway RTO is that optimal paths are insensitive to takeoff weights within a certain range. Figures 7 and 8 show the RTO paths with $h_0 = 20$ ft for four takeoff weights selected from Tables 1 and 2, where Table 2 is based on Ref. 26. Except for $W = 15,479$ lb, the minimum runway lengths are about the same. Runway field lengths are about the same as well with $h_0 = 10$ ft. These results are consistent with the flight tests reported in Ref. 3.

Figures 7 and 8 also show the basic features of minimum runway RTO flights. A typical RTO flight path consists of three phases. The first phase is a transition from a takeoff climb to a steady descent. The thrust coefficient drops to zero level; indicating the need to reduce collective upon the decision to land. Correspondingly, the rotor speed increases to the upper limit. The helicopter stores energy in its rotor. The

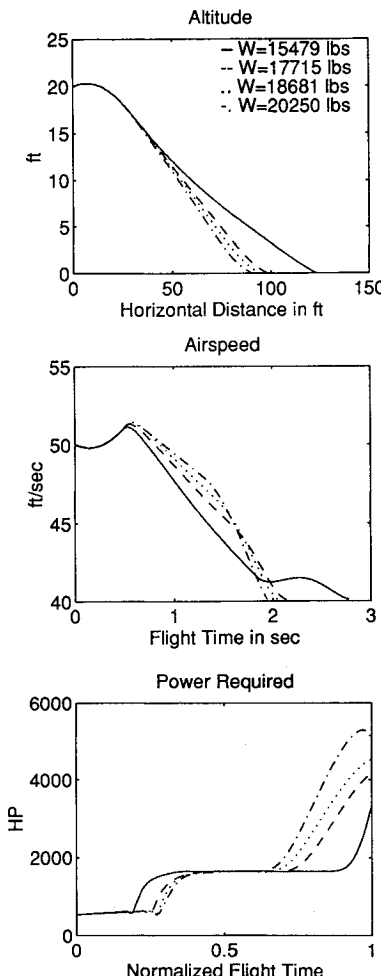


Fig. 7 Effect of weight in OEI minimum runway length RTO.

Table 2 Typical mission weights for UH-60 helicopter

Condition	Weight, lb
Aeromedical mission	15,479
Basic structure design	16,331
Aerial recovery mission	20,250

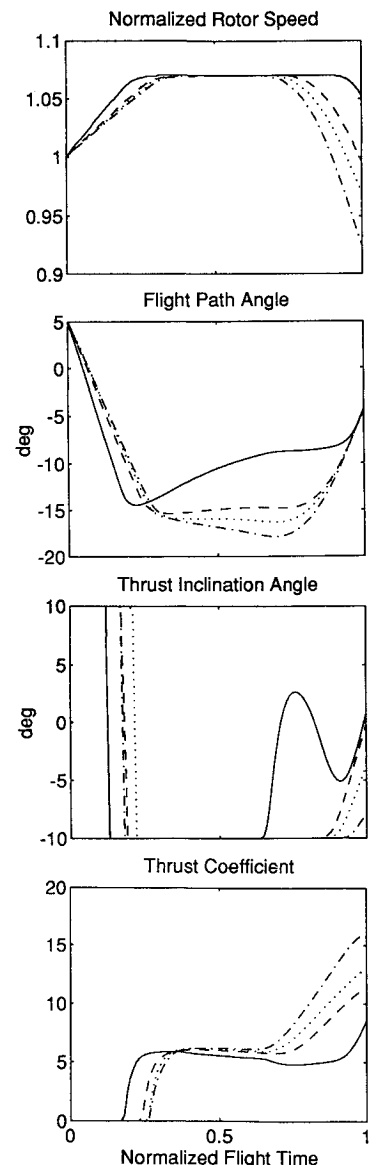


Fig. 8 Minimum runway length RTO with $V_0 = 50$ ft/s, $\gamma_0 = 5$ deg, $h_0 = 20$ ft, and different weights.

second phase of RTO is a steady descent, where the rotor speed stays at the upper limit while the helicopter power required is equal to the OEI power available. Thrust increases to a level needed to maintain the steady descent while tilting backwards to slow the helicopter down in the horizontal direction. Because the thrust is zero during the first flight phase, the thrust inclination angle can be assumed to be -10 deg. As a result, the pilot can tilt the thrust vector backwards at the maximum possible angle during both the first and the second phases of the RTO flight. In the final descent phase, the helicopter uses the energy stored in the main rotor to cushion the landing; causing thrust to increase and the rotor speed to decrease. Use of the maximum rotor speed constraint also limits the flight path angle, and thus, vertical descent

Table 3 Maximum weights in RTO with $V_0 = 50$ ft/s and $\gamma_0 = 5$ deg

h_0 , ft	W_{\max} , lb	$x_{f,rto}$, ft
10	23,102	88.31
15	22,264	94.13
20	21,651	114.04
25	21,266	133.04
30	21,033	152.55

rate. In all cases computed, the helicopter stays out of the vortex-ring state.

In RTO flights, the terminal inequality constraints in Eqs. (53) and (54) sometimes become equalities. We also compute suboptimal RTO trajectories assuming both of these terminal constraints as equalities. Results indicate that these trajectories are very similar to the optimal trajectories where Eqs. (53) and (54) are enforced as inequalities.

B. Maximum Takeoff Weight in RTO

Actually, there is a finite range of takeoff weights within which the minimum runway length is insensitive to takeoff weight. As the takeoff weight becomes smaller, the minimum runway length increases slightly (Fig. 7). When the takeoff weight is further reduced, the optimization problem can fail to converge; suggesting that it may be difficult to land a too light-weighted helicopter.

When the takeoff weight becomes too large, on the other hand, the optimization problem fails to converge as well. Physically, there is a maximum safe weight in RTO for each set of initial conditions. We can determine these maximum weights through the following optimization problem:

$$\min I = \delta \quad (55)$$

subject to Eqs. (26–36), and Eqs. (52–54). There is no constraint on the final horizontal distance. Table 3 shows the maximum weights possible in RTO and the corresponding runway lengths required, as functions of engine failure height for $V_0 = 50$ ft/s and $\gamma_0 = 5$ deg.

The maximum weight for RTO varies with V_0 and γ_0 . For $50 \leq V_0 \leq 80$ ft/s, maximum RTO weights are between 21,000–22,000 lb. Therefore, the maximum takeoff weight in a Category-A runway takeoff is determined by continued takeoff and climbout (Table 1).

VI. Conditions of Takeoff Decision Point

We now combine the results of continued takeoff and rejected takeoff to obtain insights on the choice of TDP conditions. Figure 9 shows the minimum runway field lengths required for RTO and CTO for $V_0 = 50$ ft/s, $W = 17,715$ lb, and $\gamma_0 = 5, 7$, and 9 deg. Results for other values of V_0 can be similarly constructed. Total runway lengths required are calculated from

$$X_{CTO} = \frac{V_0^2}{0.4 g} + \frac{h_0 - 5'}{\tan \gamma_0} + x_{f,cto} \quad (56)$$

$$X_{RTO} = \frac{V_0^2 + u_{\max}^2}{0.4 g} + \frac{h_0 - 5'}{\tan \gamma_0} + x_{f,rto} \quad (57)$$

We can use Fig. 9 to select TDP heights. A balanced field length (BFL) results when both RTO and CTO require the same runway length. To achieve a BFL for $V_0 = 50$ ft/s, $\gamma_0 = 5$ deg, and $W_{\max} = 17,715$ lb, e.g., we have $h_{TDP} = 24$ ft. As γ_0 increases, TDP height for balanced field length and the corresponding BFL both decrease. Figure 9 can also be used to determine the best TDP height for unbalanced field length cases, as required in some heliport configurations.

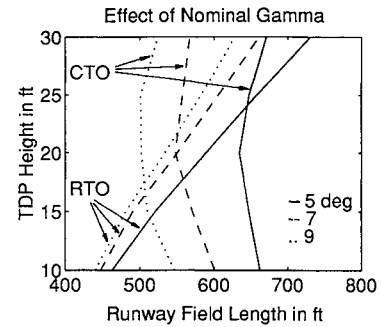


Fig. 9 Minimum runway lengths for $V_0 = 50$ ft/s, $W = 17,715$ lb, and $U_2 = 65$ ft/s (for CTO).

Choice of V_0 on the nominal AEO takeoff path affects the maximum takeoff weight capability and runway length. Since the maximum takeoff weight is determined by CTO, a higher V_0 results in a higher payload capability at the expense of a longer runway length.

While TDP conditions establish decision criteria on continuing or rejecting the takeoff in the event of one engine failure, actual engine failures may occur at any height. Continued takeoff becomes easier as the engine failure height increases beyond the TDP height, while rejected takeoff becomes easier as the failure height decreases below the TDP height. One could maximize flight safety in either case. For simplicity, one can just follow the minimum runway length flight trajectories.

Future work will use a six degree-of-freedom rigid-body helicopter model and expand the investigation to include the effects of c.g. travel, pitch attitude constraints, g-loading constraint, and the pilot response time.

VII. Conclusions

Extensive trajectory optimizations are conducted to examine basic features of multiengine helicopter runway takeoffs in the case of one engine failure. Both continued takeoff and rejected takeoff flight are investigated. Two optimal control problems are formulated. Subject to specified final conditions, one formulation minimizes the runway field length for a given takeoff weight and the other maximizes the takeoff weight. Numerical results replicate those from flight tests reported in the literature.

In a continued takeoff, a helicopter trades rotational energy for potential and kinetic energy. As a result, the rotor angular speed reduces to and stays at the lower limit for a substantial part. An optimal choice of the takeoff safety speed is about 15 ft/s or 10 kn above the nominal takeoff speed. This choice maximizes the takeoff weight while the helicopter monotonically gains altitude during the continued takeoff following an engine failure. The problem of minimizing runway length for a given takeoff weight produces nearly identical trajectories as that of maximizing the takeoff weight for a fixed runway length, if the weight and runway length are properly specified.

In a rejected takeoff, a helicopter stores energy in the rotor at the beginning and uses this rotational energy to soften the landing at the end. As a result, the rotor speed reaches the maximum limit during the steady descent. The minimum runway length is relatively insensitive to takeoff weights that are less than the maximum weight possible for given initial conditions.

Combined considerations of continued and rejected takeoff shed light on the choices of TDP conditions. For obtaining BFL, TDP height decreases for increased nominal flight-path angle. Maximum takeoff weights in Category-A runway operations are determined by continued takeoff. To increase the maximum takeoff weight capability, larger nominal takeoff speeds can be used, at the expense of longer runway field lengths.

Appendix: UH-60A Parameters for Optimization Studies

The UH-60A helicopter has a maximum takeoff weight of 22,000 lb. The maximum takeoff power is 3086 shaft hp. Other related parameters are $R = 26.83$ ft, $\sigma = 0.0821$, $\Omega_0 = 27$ rad/s, $C_{T_{\max}} = 0.01846$, and $I_R = 7060$ slug ft².

Values of parameters used in the optimizations are $f_e = 30$ ft², $\rho = 0.002377$ slugs/ft², $g = 32.2$ ft/s², $c_d = 0.012$, $\eta = 0.85$, $K_{\text{ind}} = 1.15$, $W_0 = 20,000$ lb, $w_{\max} = 3$ ft/s, and $u_{\max} = 40$ ft/s, $\beta_{\max} = 10$ deg, $\bar{\Omega}_{\max} = 107\%$, $\bar{\Omega}_{\min} = 91\%$, $P_{\text{accessory}} = 47.3$ hp, $P_{\text{OEI},110\%} = 1650$ hp, $P_{\text{OEI},105\%} = 1573$ hp.

Acknowledgments

This work was completed when the first author visited Ames Research Center during January to March, 1994. The work is supported through a cooperative agreement between NASA Ames Research Center and the University of Minnesota under NCC2-809. We thank Supercomputer Institute at the University of Minnesota for granting its supercomputer resources. We thank William S. Hindson at NASA Ames for many helpful discussions.

References

- ¹Certification of Transport Category Rotorcraft, Federal Aviation Administration, Advisory Circular AC-29A, 1987.
- ²Cerbe, T., and Reichert, G., "Optimization of Helicopter Takeoff and Landing," *Journal of Aircraft*, Vol. 26, No. 10, 1989, pp. 925-931.
- ³Saal, K. W., and Cole, J. L., "Category 'A' Certification of S-76B Featuring Variable CDP and V2 Speeds," *Journal of the American Helicopter Society*, Vol. 35, No. 3, 1990, pp. 12-21.
- ⁴Okuno, Y., and Kawachi, K., "Optimal Takeoff of a Helicopter for Category A STOL/VTOL Operations," *Journal of Aircraft*, Vol. 30, No. 2, 1993, pp. 235-240.
- ⁵Vodegel, H. J. G. C., and Stevens, J. M. G. F., "A Computer Program for the Certification of Helicopter Vertical Takeoff and Landing Operations and an Application to the S-76B Helicopter," *Proceedings of the 47th Annual Forum of the American Helicopter Society* (Phoenix, AZ), American Helicopter Society, 1991, pp. 721-731.
- ⁶Goldenbarg, J., Meslin, L., Blondino, M., and Williams, D., "Certification of Model 230 Helicopter for Category 'A' Elevated Helipad Operations," American Helicopter Society 49th Annual Forum, St. Louis, MO, May 1993.
- ⁷Lande, K., "New Offshore Helicopter Rig Takeoff and Landing Procedures," *Proceedings of the 1989 Experimental Test Pilot Symposium* (Beverly Hills, CA), 1989, pp. 179-204.
- ⁸Johnson, W., "Helicopter Optimal Descent and Landing After Power Loss," NASA TM 73244, May 1977.
- ⁹Lee, A. Y., Bryson, A. E., and Hindson, W. S., "Optimal Landing of a Helicopter in Autorotation," *Journal of Guidance, Control, and Dynamics*, Vol. 11, No. 1, 1988, pp. 7-12.
- ¹⁰Okuno, Y., Kawachi, K., Azuma, A., and Saito, A., "Analytical Prediction of Height-Velocity Diagram of a Helicopter Using Optimal Control Theory," *Journal of Guidance, Control, and Dynamics*, Vol. 14, No. 2, 1991, pp. 453-459.
- ¹¹Talbot, P. D., Tinling, B. E., Decker, W. A., and Chen, R. T. N., "A Mathematical Model of a Single Main Rotor Helicopter for Piloted Simulation," NASA TM-84281, Sept. 1982.
- ¹²Johnson, W., *Helicopter Theory*, Princeton Univ. Press, Princeton, NJ, 1980, pp. 282, 283.
- ¹³Hirschkron, E., Martin E., and Samanich, N., "Powerplant Design for One Engine Inoperative Operation," *Vertiflite*, Vol. 30, No. 5, 1984, pp. 34-38.
- ¹⁴Schmitz, F., *Aerodynamics of Helicopters*, AA 230 Class Notes, Stanford Univ., Stanford, CA, 1991.
- ¹⁵Gessow, A., and Myers, G. C., Jr., *Aerodynamics of the Helicopter*, Frederick Ungar Publishing, New York, 1952.
- ¹⁶Stepniewski, W. Z., and Keys, C. N., *Rotary-Wing Aerodynamics*, Dover, New York, 1984.
- ¹⁷*Operator's Manual: UH-60A and EH-60A Helicopters*, Dept. of the Army, TM 55-1520-237-10, Jan. 1988.
- ¹⁸Howlett, J. J., "UH-60A Black Hawk Engineering Simulation Program," Vol. I, NASA CR-166309, Dec. 1981.
- ¹⁹Prouty, R. W., *Helicopter Performance, Stability, and Control*, Krieger, Malabar, FL, 1990, p. 698.
- ²⁰Hilbert, K. B., "A Mathematical Model of the UH-60 Helicopter," NASA TM 85890, April 1984.
- ²¹Schmitz, F., "Optimal Takeoff Trajectories of a Heavily Loaded Helicopter," *Journal of Aircraft*, Vol. 8, Nov. 9, 1971, pp. 717-723.
- ²²Chen, R. T. N., "A Survey of Nonuniform Inflow Models for Rotorcraft Flight Dynamics and Control Applications," NASA TM 102219, Nov. 1989, p. 48, Fig. 24.
- ²³Jacobson, D. H., and Lele, M. M., "A Transformation Technique for Optimal Control Problems with a State Variable Inequality Constraint," *IEEE Transactions on Automatic Control*, Vol. AC-14, No. 5, 1969, pp. 457-464.
- ²⁴Miele, A., Damoulakis, J. N., Cloutier, J. R., and Tietze, J. L., "Sequential Gradient Restoration Algorithm for Optimal Control Problems with Non-Differential Constraints," *Journal of Optimization Theory and Applications*, Vol. 13, No. 2, 1974, pp. 218-255.
- ²⁵Anon., "Supa Puma MK2 Supplement for Category A Operations," undated Flight Manual.
- ²⁶*Black Hawk Helicopter*, Sikorsky Aircraft, Table 4.2, p. 4.8.